



Using computed tomography images to characterize the effects of soil compaction resulting from large machinery on three-dimensional pore characteristics in an opencast coal mine dump

Yu Feng¹ · Jinman Wang^{1,2}  · Tao Liu¹ · Zhongke Bai^{1,2} · Lucy Reading³

Received: 23 August 2017 / Accepted: 3 September 2018 / Published online: 8 September 2018
© Springer-Verlag GmbH Germany, part of Springer Nature 2018

Abstract

Purpose The use of heavy machinery in mining areas increases during mining and dumping of waste soils, causing severe soil compaction and potentially affecting soil recovery. This study aimed to capture the features of complex compacted soil pore structure using computed tomography (CT) and to quantify soil pore distribution properties based on Minkowski theory.

Materials and methods A total of 45 cylindrical soil columns were extracted from different soil layer at 5 sampling sites that differed in compaction level in Pingshuo opencast coal mine in Shanxi Province of China. The penetration resistance at these sites ranged from 27.3 to 1023.1 kPa. Three-dimensional reconstruction software VGStudio was used to obtain the morphological characteristics (pore volume density, VD; surface density, SD; mean curvature density, MCD; and Euler number, EN) of soil pores after processing the X-ray scanned image.

Results and discussion Compaction generally reduced VD, SD, and MCD, which ranged from 0.10 to 0.20, 2.23 to 2.80 mm² mm⁻³, and 10.75 to 15.64 mm mm⁻³ respectively in undisturbed site P0, whereas, they ranged from 0.02 to 0.07, 0.13 to 0.60 mm² mm⁻³, and 1.61 to 4.27 mm mm⁻³ respectively in highly compacted site P4. The three index exhibited the similar trend, and decreased with the increase of compaction level. Soil compaction had positive effects on EN, which was low at the depth of 20- to 40-cm layers but showed an increasing trend with increasing soil compaction level. The value of EN varied from 28,878 to 129,861 in P0, whereas it varied from 1,169,967 to 2,281,998 in P4.

Conclusions All of macroporosity, mesoporosity, and microporosity were significantly affected by heavy machinery compaction, among which macroporosity exhibited the maximum decrease in P4 compared to that in P0 (P0 ranged from 14.2 to 26.4% and P4 ranged from 0.2 to 1.4%). The soil compaction in mining area significantly affected soil properties, thus artificial methods such as fertilizer application and deep tillage were needed.

Keywords CT image · Land reclamation · Minkowski functional · Opencast coal mine · Soil compaction · Soil reconstruction

Responsible editor: Yi Jun Xu

✉ Jinman Wang
wangjinman@cugb.edu.cn

- ¹ College of Land Science and Technology, China University of Geosciences, 29 Xueyuan Road, Haidian District, Beijing 100083, People's Republic of China
- ² Key Laboratory of Land Consolidation and Land Rehabilitation, Ministry of Land and Resources, Beijing 100035, People's Republic of China
- ³ School of Earth, Environmental and Biological Sciences, Science & Engineering Faculty, Queensland University of Technology, 2 George Street, GPO Box 2434, Brisbane 4000, Australia

1 Introduction

Opencast coal mining activities result in severe degradation of land resources and ecological environment (Wang et al. 2016). In the process of opencast mining, topsoil overlying the coal are stripped and deposited on dam-like dump with large-scale heavy machinery (Krummelbein et al. 2010). The compaction effects are intensified by the large tires of crawlers and dump trucks going back and forth. As a result, compacted areas often show poor soil functionality and productivity (Horn et al. 1995; Mueller et al. 2010). The soil compaction causes a hidden degradation of soil pore structure that is difficult to evaluate (McGarry and Sharp 2003). As the size, shape, and continuity of soil pores affect water, solutes, and gas exchange processes (Greacen and Sands 1980; Soracco et al. 2015),

structural changes of compacted soil pores may affect these processes and reduce the soil biological activity of flora and fauna (Beylich et al. 2010). Thus, the pore properties of compacted soil play an important role in land reclamation in opencast mining areas.

Previous research on soil compaction has focused on specific aspects such as the physical influence (Horn et al. 1995), organic matter (Soane 1990), and modeling (Osullivan and Simota 1995; Lipiec and Hatano 2003). The anthropogenic causes of soil compaction can occur due to agricultural operations from sowing to harvesting (Williamson and Neilsen 2000), grazing animals trampling and visitors pressure (da Silva et al. 2003; Frick et al. 2007), which frequently take place in cultivated lands, forests and urban parks (Nawaz et al. 2013). The effects of vehicle traffic on soils have been long and intensively investigated. Previous studies have demonstrated that under these conditions, soil bulk density increases, and macroporosity and hydraulic conductivity decreases for surface soils (Taylor 1992; Worrell and Hampson 1997; Xu et al. 2002). However, large mechanical recycling operations result in much more significant soil compaction in mining areas (Shukla et al. 2004), compared with the compaction that takes place in the cultivated lands or forests. Because of the rolling action of the heavy machinery, the level of soil compaction and depth to which compaction occurs are much larger in mining areas than in agricultural areas.

The level of soil compaction can be affected by several factors such as soil texture, moisture content, tire load, and the number of times that the machinery passes (Oni and Adeoti 1986; Dauda and Samari 2002). The soil physical parameters that are most sensitive to compaction are bulk density, porosity, and penetration resistance (Panayiotopoulos et al. 1994; Hamza and Anderson 2003; Barik et al. 2011). Traditionally, the soil–water retention method, measured in the laboratory, has been widely used to characterize soil porosity and analyze soil pore structure (Vogel 2000; Rachman et al. 2005; Amer et al. 2009; Wang et al. 2016). However, laboratory methods can only provide indirect information about soil pore structure (Schluter et al. 2016). Advances in the application of computed tomography (CT) for measuring pore size, volume, and surface area, and pore connectivity have provided a new research tool for thorough investigation into the compacted soil pores (Udawatta et al. 2008; Kumar et al. 2010; Rab et al. 2014). Computed tomography is a non-invasive imaging technique that proved to be powerful to visualize and quantify soil pore structure (Taina et al. 2008; Cortina-Januchs et al. 2011). X-ray CT method may provide a better understanding of soil pore structure and how the process of soil dumping and large machinery compaction may influence soil processes. Over the last few decades, X-ray CT has been increasingly used in geosciences (Cnudde and Boone 2013) and soil science (Taina et al. 2008) to investigate the spatial distribution of sediment particles and pore spaces

(Goodwin et al. 2003). Most studies have been focused on the evaluation of soil pore structure, particularly on macroporosity and density investigations (Warner et al. 1989; Anderson et al. 1990; Lipiec and Hatano 2003). Today various tomographic techniques are available for three-dimensional visualization of soil pore structure properties (Katuwal et al. 2015; Meng et al. 2017). For a better description of compacted soil pore structure, geometrical characteristics such as pore volume, surface area, and connectivity are analyzed. Mathematical morphology is a well-established technique and provides an efficient way to characterize the geometric information of different features of soil pore structure that can be obtained through X-ray CT (San José Martínez et al. 2016). Among the tools of mathematical morphology, the Minkowski method is particularly efficient for measuring the three-dimensional soil pore space (Arns et al. 2002; Lehmann et al. 2006).

The impact of agricultural soils compaction has been extensively studied, but few have been focused on highly compacted dump soils. A few studies have been conducted on reclaimed soil using CT method (Wang et al. 2016; Wang et al. 2017a). However, the previous studies focused on the duration of reclamation period on soil pore properties and the two-dimensional image analysis. Very limited information is available for measuring pore characteristics of compacted soil using traditional methods. Despite the value of CT as a technique for understanding the impacts of compaction on soil porosity and subsequent implications for soil restoration, the morphological characteristics of soil pores is still not well quantified, including pore size, volume, surface area, and connectivity. Therefore, the objectives of this study were to (i) compare Minkowski theory for determining pore characteristic parameters with traditionally used CT parameters and (ii) compare soil pore distribution characteristics under different level of compaction resulted from heavy machinery.

2 Materials and methods

2.1 Study area

The study area was located in Pinglu District of Shuozhou City, Shanxi Province, which has the largest opencast coal mine (112° 17' 28"~112° 28' 10" E, 39° 25' 6"~39° 36' 5" N) in China and includes the Antaibao, Anjialing, and East opencast mines. The specific study area was the dump site located in one of the Pingshuo opencast mines, Antaibao. With an area of 376 km², Antaibao opencast mine contains the three large dumps, the South, the West, and the Inner Dump. Better eco-landscape had been formed on the South and West Dump, with 23 and 20 years of reclamation. The Inner Dump, with an area of 0.44 km² and no reclamation after dumping, was selected as the sampling site in this study.

The study area has a typical temperate arid to semi-arid continental monsoon climate and a fragile ecosystem. The average altitude is approximately 1400 m, while the altitude difference in mine area can be 300 m. The soil type is chestnut soil. The soils have low soil organic matter content, poor soil structure, and weak resistance to water erosion and wind erosion (Bai et al. 1998). Without good vegetation cover, this area has suffered from soil erosion for many years which has caused further deterioration in soil conditions in this mining area.

Opencast coal mining, including excavating, transporting, and dumping, has significantly disturbed the topsoil and changed the soil profile (Wang et al. 2017b). At the beginning of mining, 0–100 cm of topsoil was moved and stored separately. After transporting and dumping, the removed topsoil was used to cover the surface of the dump, and some areas have been used for agriculture (Li et al. 2012). Although land reclamation began 20 years ago in Pingshuo opencast mine (Bi et al. 2010), large machinery caused severe compaction on these dumps, which made the reclamation a longer process.

2.2 Soil sampling

Four sampling sites representing different compaction levels, i.e., P1, P2, P3, and P4, were selected to analyze the effects of soil compaction based on the level of compaction, and the undisturbed soil site, P0, was set as the control site (Fig. 1). The penetration resistance of different sampling sites are presented in Table 1. At each sampling sites, a 5 m × 5 m area was marked and three profiles were selected randomly within this area. Soil samples were collected from each soil profile at the depths of 0–20 cm, 20–40 cm, and 40–60 cm, and a total of 45 soil samples (30 mm in diameter and 60 mm in height) were collected. First, an acrylic cylinder was put into the soil by gradually pressing a pedestal with the hand shank on it. Then, a backhoe was used to carefully remove the soil from around the column and push the acrylic cylinder deeper into the soil before later removing the column slowly. The soils protruding from the top and bottom of the extracted acrylic cylinder were cut (San José Martínez et al. 2010). This sampling procedure provided gradual penetration of the column into the soil with minimum disturbance of soil core. The soil core was wrapped with cling wrap and aluminum foil and kept at 2 °C until CT scanning (Naveed et al. 2016).

At each soil core location, an additional soil sample was collected at corresponding depth for analysis of soil bulk density (BD) and penetration resistance (PR). Mean values of BD and PR for five sampling sites at three soil depths are presented in Table 1. The soil bulk density

(BD) of each soil sample was determined by the cutting ring method (Blake and Hartge 1986). A penetration resistance tester (TJSD-750, Zhejiang Top Instrument Co., Ltd., Hangzhou City, Zhejiang Province, China) was used at P0, P1, P2, P3, and P4.

2.3 CT scanning and image processing

The soil cores were scanned in helical mode at the Aerospace Research Institute of Special Materials & Processing Technology of China in July 2015. The CT scanner is an X-ray digital core analysis system (GE Measurement & Control, German Phoenix Company, German). In this study, the helical scanning mode was used to make a relatively quick precision enhancement of the image. Each soil column was placed horizontally on the couch of the CT scanner, so the original soil profile was perpendicular to the X-ray plane. The CT scanning configuration parameter values were as follows: tube voltage, 180 kV; pixel size of the flat panel detector, ≤ 50 μm; number of pixels, 2200 × 2200; pixel size of the minimum element, < 0.5 μm; field of view, 12 cm in diameter and 15 cm in height; and image reconstruction interval length, 0.05 mm. Only the middle part of the soil column was scanned and the region between 5 and 55 mm was selected for the image processing. The resolution of scanned images was 18 μm, and the scanning interval was a continuous 0.05 mm. The images were analyzed using the Image J 2 software, and the Region of Interest (ROI) tool was used to exclude voids near the core walls and minimize the effects of beam hardening (Schneider et al. 2012). Soil pore was partitioned from solid using the Threshold tool after converting the image into an 8-bit grayscale image. Conversion of the image included all of the original data, and the known phantoms on the sample were used to validate the conversion. Image segmentation was the most crucial step affecting all subsequent quantitative analysis efforts (Iassonov et al. 2009). Various classification schemes for image segmentation methods were proposed in literature (Haralick and Shapiro 1985; Pal and Pal 1993; Sezgin and Sankur 2004), and errors and distortions were inevitable during the segmentation process. Among different approaches of image segmentation, histogram thresholding was commonly applied (Rachman et al. 2005). A value of 60 (range is 0–255) was selected as the threshold to conduct image analysis; the value was determined using optimization with known phantoms which included air-filled and water-filled tubes. The values less than the threshold value were identified as air-filled or water-filled pores and the values greater than the threshold value were identified as non-pore.

VGStudio, a well-performed three-dimensional display software, was used to observe the internal structure of the soil pores. First, the scanned CT images were imported into VGStudio, and the three-dimensional soil column was obtained. Then, after the eliminating of exterior plexiglass tube part,

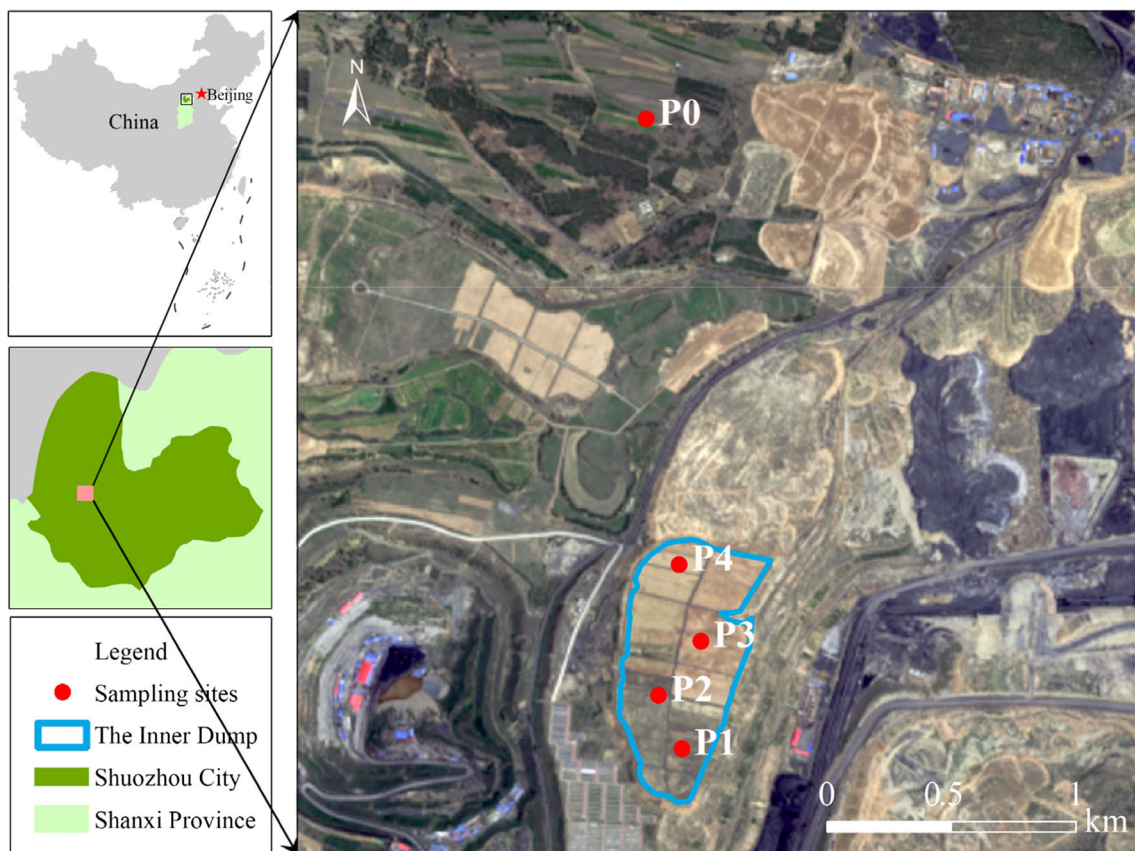


Fig. 1 Location of study area and sampling sites

selected areas were extracted by the Extracted.roi menu item. Finally, considering the memory space of the computer and elimination the images on the top and bottom parts of the soil acrylic cylinder to avoid any artificial disturbance during sampling, a total of 1000 images were imported into the software to make soil column reconstruction. The reconstructed soil column was cylindrical, with the height of 50 mm, the diameter of 30 mm and the voxel size of $18 \mu\text{m} \times 18 \mu\text{m} \times 18 \mu\text{m}$. The CT scanning images processing and three-dimensional reconstruction workflow are shown in Fig. 2.

The equivalent diameter (ED) of each pore was calculated by the following equation (Rasiah and Aylmore 1998):

$$ED = 2\sqrt{\frac{A}{\pi}} \quad (1)$$

where A is the soil pore area in soil cross-section in μm^2 . Due to the limitation of the image resolution, only the soil pores with $ED \geq 18 \mu\text{m}$ were studied in this paper, and the pore size were divided into three categories (Bouma et al. 1977; Beven 1981; Luxmoore 1981), macropores ($ED \geq 100 \mu\text{m}$), mesopores ($30 \mu\text{m} \leq ED \leq 100 \mu\text{m}$), and micropores ($18 \mu\text{m} \leq ED \leq 30 \mu\text{m}$).

2.4 Characterization of three-dimensional soil pore distribution

Minkowski functionals are basic geometric measures defined for binary structures (Vogel et al. 2010) and can be used to quantify the measured pore structure. After segmentation, the pore space is represented as a binary structure $X \subset \Omega$ where Ω

Table 1 Mean soil bulk density and penetration resistance of the sampling sites

Soil depth (cm)	Bulk density (BD) (Mg m^{-3})					Soil depth (cm)	Penetration resistance (PR) (kPa)				
	P0	P1	P2	P3	P4		P0	P1	P2	P3	P4
0–20	1.42	1.65	1.68	1.76	1.85	0–20	27.3	487.3	612.2	740.1	893.9
20–40	1.48	1.62	1.64	1.71	1.73	20–40	63.1	350.7	459.2	573.6	1023.1
40–60	1.54	1.69	1.73	1.79	1.88	40–60	105.8	189.4	234.6	395.5	503.0

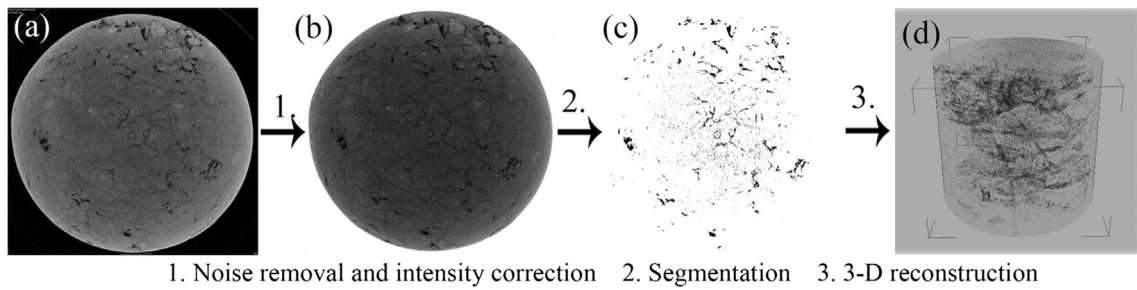


Fig. 2 Image processing workflow and 3-D reconstruction of soil pores **a** original image, **b** enhanced image, **c** binarized image, **d** three-dimensional visualization of sample soil column

is the embedding space (i.e., a three-dimensional image of any shape to be analyzed) and X is the pore space. Given such a binary image, integral geometry provides a limited set of $d + 1$ Minkowski functionals (Mecke 2000), where d is the dimension of Ω , in our case $d = 3$. Basic geometric characteristics are likely to be related to functional aspects of material (Vogel et al. 2010), and the pore volume, surface area, mean curvature, connectivity, and Euler number were used in this study. The first functional M_0 is the total volume of pores:

$$M_0(X) = V(X) \tag{2}$$

Other Minkowski functionals are defined through integrals over the surface of the pores denoted as ∂X which unambiguously defines its shape or morphology of the pore structure at the given resolution. In d -dimensional space, there are d such integrals. For $d = 3$, the first integral measures the total interfacial area between pore and solid:

$$M_1(X) = \int_{\partial X} ds = S(X) \tag{3}$$

where ds is a surface element. The second integral measures the mean curvature:

$$M_2(X) = \frac{1}{2} \int_{\partial X} \left[\frac{1}{r_1} + \frac{1}{r_2} \right] ds = C(X) \tag{4}$$

where r_1 and r_2 are the minimum and the maximum radius of curvature for surface element ds , respectively.

In addition, for a better understanding of soil pore structure and hydraulic properties, Euler number (EN) can be a suitable parameter to quantify the topological relations of soil pores and an increasing Euler number indicates the decreasing connectivity of them. The EN can be calculated using the classical Euler formula (Vogel et al. 2010).

EN is a dimensionless, topological measure that quantifies the connectivity of the pattern while M_0 , M_1 , and M_2 are metric with units $[L^3]$, $[L^2]$, and $[L]$, respectively.

In order to compare the results obtained from different images, normalization is needed to remove the effect of image size. Minkowski densities are averaged properties without information on pore size distribution. Thus, the Minkowski densities were calculated using the following equation:

$$m_k(X) = \frac{M_k(X \cap \Omega)}{V_\Omega} \tag{5}$$

The physical interpretations of these functionals are the following: m_0 corresponds to the total volume of pores, m_1 corresponds to surface area, m_2 is related to pore shape, and EN is related to soil connectivity. Minkowski densities represent properties of soil pore structure and can be calculated using an algorithm based on the binary image (Vogel et al. 2010). Thus, the three-dimensional characteristic parameters in this study are volume density (VD), surface density (SD), mean curvature density (MCD), and Euler number (EN).

2.5 Statistical analysis

One-way ANOVA was used to perform significance test, and the differences of characteristics parameters of soil pore distribution among five different soils (P0, P1, P2, P3, and P4) at the depths of 0–20, 20–40, and 40–60 cm were compared at the P value of 0.05. Correlation analyses were conducted among soil three-dimensional feature parameters. All the statistical analyses were conducted using SPSS20.0 software (SPSS, Chicago, USA).

3 Results

3.1 Three-dimensional feature parameters of soil pores

Based on VGStudio MAX 2.0 software, the three-dimensional reconstructed pore structure of tested soils was depicted in Fig. 2. The visual observations of the reconstructed soil pore structure indicated significant differences among not only sampling points but also soil layers. Reconstructed soil pore features include three-dimensional pore volume, surface area, mean curvature, and connectivity.

3.1.1 Volume density (VD)

The three-dimensional pore VD quantifies pore volume features, which can be represented by a binary image after segmentation. The greater the pore volume density is, the larger the pore volume will be. VD decreased with the increase of soil compaction level (from P1 to P4) (Fig. 3a). VD exhibited significant differences between both different compacting levels and different soil depths ($P < 0.05$). The values of total volume density at the layers of 0–20 cm, 20–40 cm, and 40–60 cm in P1, P2, P3, and P4 showed the same trend: $VD_{L2} > VD_{L1} > VD_{L3}$. This order was in agreement with the penetration resistance results tested from shallow to deep soil profile for the same depths. Compared with P0 at layers of 0–20 cm, 20–40 cm, and 40–60 cm (with 0.20, 0.13, and 0.10 respectively), VD of P4 were lower (with 0.04, 0.07, and 0.02 respectively). Moreover, a different order was exhibited in P0, $VD_{L1} > VD_{L2} > VD_{L3}$, which indicated the difference between undisturbed landforms and the compacted sites.

3.1.2 Surface density (SD) and mean curvature density (MCD)

SD and MCD exhibited similar trend with pore VD, and both were statistically significant ($P < 0.05$). Values of SD and MCD at 20- to 40-cm layers were the highest at compacted sampling sites, whereas those at 0- to 20-cm layers of undisturbed sites have the highest value (Fig. 3b, c). SD ranged from 2.23 to 2.59 $\text{mm}^2 \text{mm}^{-3}$ at undisturbed sites P0 and ranged from 0.13 to 0.60 $\text{mm}^2 \text{mm}^{-3}$ at highly compacted sites P4. MCD of P0 varied from 10.75 to 15.64 $\text{mm} \text{mm}^{-3}$ and that of P4 varied from 1.61 to 4.27 $\text{mm} \text{mm}^{-3}$, which showed a significant difference between the two sampling sites (Fig. 3b, c).

3.1.3 Euler number (EN)

EN reflects the connectivity of soil pores. The EN exhibited differences between soils with different levels of compaction according to one-way ANOVA results ($P < 0.05$). At the undisturbed sampling site P0, EN increased as soil depth increased, while at the compacted sites (from P1 to P4), EN reached to the lowest point at 20- to 40-cm layers (i.e., $EN_{L3} > EN_{L1} > EN_{L2}$) (Fig. 3d). The value of EN also showed large differences between P0 and P4 (P0: varied from 28,878 to 129,861; P4: varied from 1,169,967 to 2,281,998).

3.2 Correlation analysis of parameters

Parameter correlation analyses were conducted and each parameter was found to exhibit significant correlation with all of the other parameters (Table 2). Correlation coefficients ranged between 0.88 and 0.99, among which there was a significantly positive correlation between surface area and mean curvature

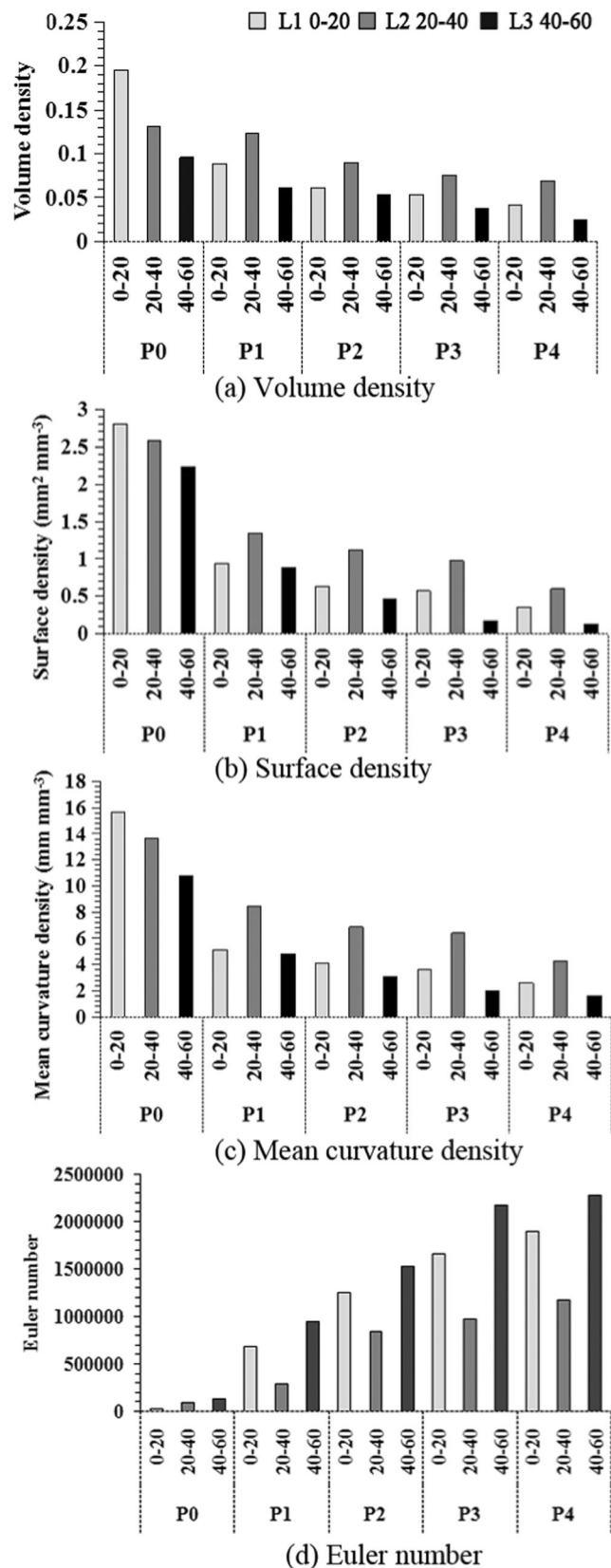


Fig. 3 Distribution of soil pore features in different layers under different pressure

Table 2 Correlation analysis of parameters

	Volume density	Surface density	Mean curvature density
Surface density	0.910**		
Mean curvature density	0.944**	0.992**	
Euler number	−0.880**	−0.902**	−0.897**

The symbol (**) in the table indicates that the correlation is significant at 0.01 level

density. However, the correlations between Euler number and other parameters were negative.

3.3 Variation in soil pore characteristics with soil depth

Variations in soil pore properties in different layers are shown in Fig. 4. The shape of the soil porosity and pore number curves of P0 differed from that of P4. Without machinery compaction, the trends of macroporosity, mesoporosity, and microporosity in P0 generally decreased as soil depth increased (values of macroporosity, mesoporosity, and microporosity varied from 14.2 to 26.4%, 5.0 to 10.8%, and 0.8 to 1.8% respectively) (Fig. 4a). However, the trends of porosities in P4 were severely compacted by large machinery, exhibiting a huge disturbance above 40-cm layer (Fig. 4e).

The macroporosity of each layer in P0 was greater than mesoporosity and microporosity, this differs from the pattern in the compacted sites, especially in P4 (Fig. 4e). Macroporosity in compacted sites P1, P2, P3, and P4 varied greatly at the depth of 20–40 cm. Moreover, pore numbers in P0 exhibited a relatively consistent trend to porosities in P0. In nearly every soil layer, micropores had a larger number than that of macropores, and the number of macropores decreased as compaction increased (macropore number in 10-cm layer drastically decreased from 1392 of P0 to 37 of P4), which indicated that macropores were more sensitive to soil compaction.

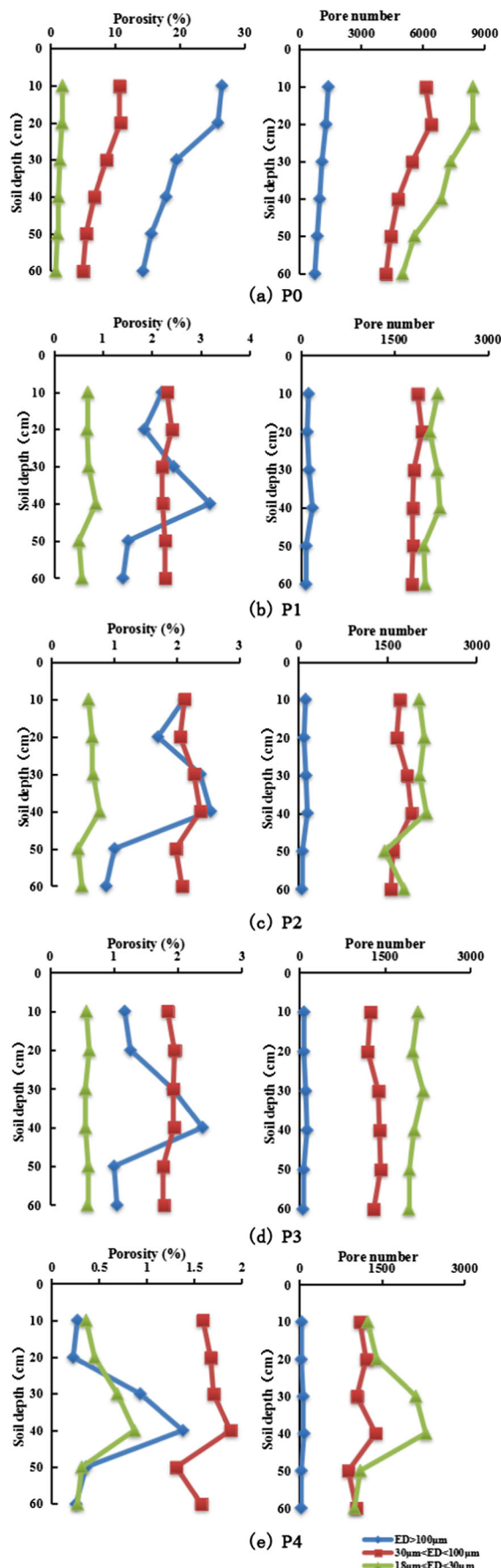
Both porosities and pore numbers showed significant differences between undisturbed sites and compacted sites (Fig. 4). As compaction level increased from P1 to P4, macroporosities varied greatly between 20- and 40-cm layers and reached to the maximum at 40-cm layer (macroporosity of P1, P2, P3, and P4 were 3.2%, 2.5%, 2.4%, and 1.4%, respectively). Mesoporosity and microporosity in compacted sites did not show a regular change; however, both showed significant differences compared with P0 (Fig. 4a). Moreover, the trends of pore numbers of different equivalent diameter almost matched with the corresponding porosity at different soil depths or under different compaction levels. For example, micropore number in P4 first increased from 1238 to 2297, and then decreased to 1001. Similar variation was also found on microporosity (increased from 0.4 to 0.7%, then decreased to 0.3%).

Figure 5 shows the distribution of soil porosity and pores at different sampling sites. From P4 to P0, total porosity and pore number of 0- to 20-cm layers ranged from 2.2 to 38.3% and 2372 to 16,133, respectively, and the orders of these two parameters are the same: P0 > P1 > P2 > P3 > P4. The order of magnitude of total porosity and pore number of 40- to 60-cm layers ranged from 4.1 to 25.8% and 3764 to 12,648. There was a trend of increased total soil porosity and an approximate trend of increased soil pores at 20- to 40-cm layer from P4 to P0, with an order of magnitude of P0 > P1 > P2 > P3 > P4 and P0 > P1 > P2 > P4 > P3, respectively (Table 3).

4 Discussion

4.1 Comparing Minkowski method with traditional CT parameters

Compaction effects on dump sites mainly caused by heavy machinery such as truck and crawler during piling up and leveling off of the substrate, resulted in severe anthropogenic impact on developing soil physical properties and functions (Krummelbein et al. 2010). In our case, not only soil physical properties such as bulk density and porosity have been used, but also Minkowski parameters, i.e., volume, surface area, mean curvature, and Euler number, have been analyzed. Bulk density is the most frequently used parameter to characterize the effects of compaction (Panayiotopoulos et al. 1994), which result in a progressive increase in bulk density and penetration resistance. The waste dumps have been compressed by large machinery, leading to high levels of compaction and high bulk densities (Barik et al. 2014). In compacted sites, bulk densities were over 1.6 Mg m⁻³ in every layer and decreased in the 20- to 40-cm layers, while bulk densities of undisturbed site P0 increased with soil depth (Table 1). Compaction resulted in increased bulk density and penetration resistance, but the correlation between these two parameters was not so close (Panayiotopoulos et al. 1994). Soil compaction results in the destruction of inter-aggregate pores, and in the reduction of soil hydraulic conductivity and air permeability (Horn et al. 1995). Under natural conditions, soil contains a large proportion of macropores. In our case, the porosity of macropores of undisturbed sites was markedly higher than that of compacted sites, and number of macropores was also significantly reduced in compacted sites compared with



◀ Fig. 4 Depth profile of soil porosity and pore number with different equivalent diameters

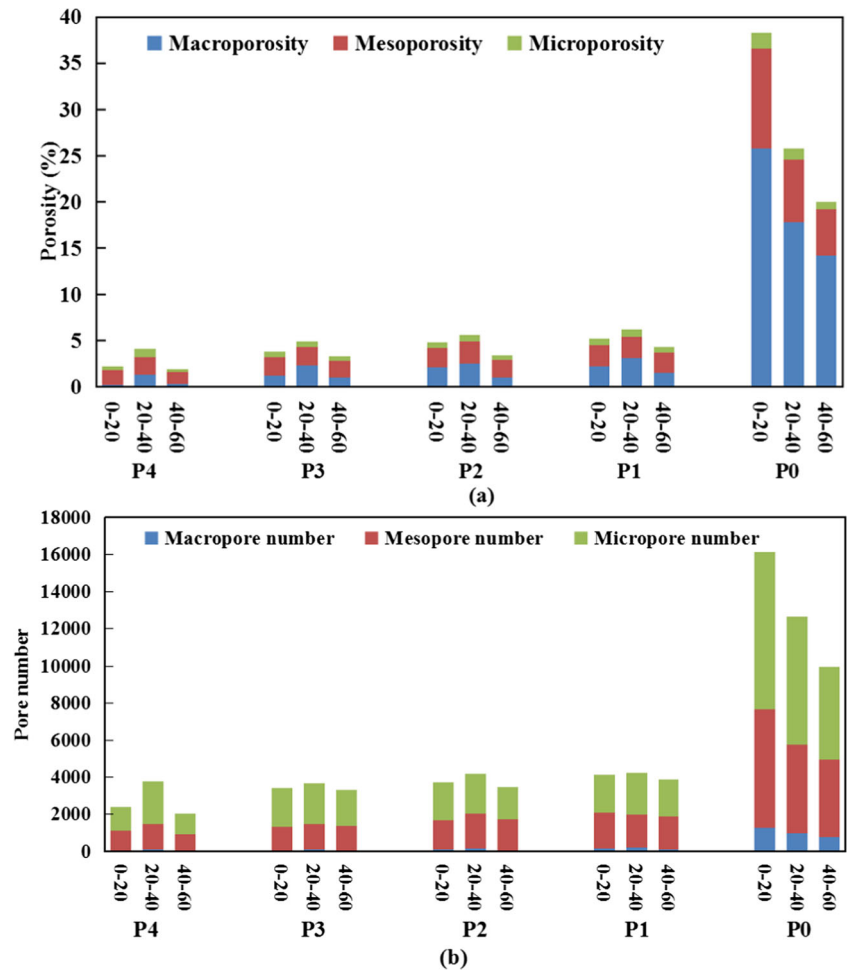
original landform (Fig. 5). The result is in accord with the observation that compaction mainly destroys large pores, and that macropores are relatively more affected by soil compaction than micropores (Nawaz et al. 2013; Soracco et al. 2015; Wang et al. 2017a).

In present study, the densities of volume fraction, surface area, and mean curvature were considered. The VD, SD, and MCD in each site presented a decreasing trend with increasing compaction level, as shown in Fig. 3a–c; whereas, Euler number showed the opposite variations and provided a sensitive measure of pore structure change in soils resulted from compaction, as shown in Fig. 3d. Differences between compacted and uncompacted soils indicated that soil compaction increased the number of isolated pores, aggravated the collapse of soil pore structure, and did not generate a complex and highly connected structure (San José Martínez et al. 2016).

4.2 Comparing traditional laboratory method with CT method

For a precise observation and evaluation on soil pore structural functions, a link between soil pore structure and physical and/or biological soil functions need to be built, which may open new avenues to evaluate the impact of soil management on mechanics and soil hydrology. However, traditional methods have limitations for the accurate characterization of soil physical features. Hence, X-ray CT is a novel technique that can be used for characterizing compacted soil pores and overcome some of the limits of traditional methods (Kim et al. 2010). Using CT images, the pores with smaller and larger equivalent diameters can be observed, thus more soil pore structural feature information can be analyzed based on Minkowski functionals such as pore volume density, surface density, mean curvature density, and Euler number (Vogel et al. 2010). The results of CT-based method and traditional method were comparable. As macropores are closely associated with the distribution of aeration and soil water, understanding the influence of soil macropore relationships on soil water flow is important for evaluating root growth and root respiration. This is typically achieved using traditional methods, which involves laboratory measurement of soil–water content at various soil–water matric potentials and inferring porosity using the relationship between pore diameter and liquid flow (Rab et al. 2014). However, as soil compaction may reduce the macroporosity and pore connectivity, the traditional methods may not be sensitive enough to detect the small changes in soil pores or other soil properties (Rab et al. 2014). In those situations, porosity as determined from traditional methods would be lower than the true value.

Fig. 5 Distribution of soil porosity and pore number at different sites



4.3 Comparing the effect of various levels of compaction due to the use of large machinery on porosity characteristics

In civil engineering, soil porosity, being independent of particle density, is widely used to measure degree of compaction (Lipiec and Hatano 2003). A decrease in soil porosity caused by compaction strongly restricts the ability of roots to access water and oxygen (Drewry et al. 2008). As macropores

determines the soil water flow and transport, macroporosity may be reduced to the extent that the growth of the roots is limited by oxygen and/or water availability. Some researchers proposed that the appropriate threshold value for the survival of plants of macroporosity is 10–15% (Lipiec and Hatano 2003). Macroporosity values in pasture compacted soils were 11.2% and 7.4% in the 0- to 10-cm and 20- to 30-cm layers respectively (Rab et al. 2014), which indicated the root growth in pasture soils may be moderately affected. In this study,

Table 3 Distribution of soil pores in different layers

Test soil	P0		P1		P2		P3		P4	
	Total porosity (%)	Pore number	Total porosity (%)	Pore number	Total porosity (%)	Pore number	Total porosity (%)	Pore number	Total porosity (%)	Pore number
10	38.9	15,955	5.2	4192	4.8	3854	3.6	3397	2.2	2372
20	38.3	16,133	4.9	4116	4.4	3861	3.8	3254	2.4	2649
30	29.5	13,905	5.4	4134	5.3	3997	4.4	3660	3.3	3226
40	25.8	12,648	6.3	4210	5.7	4207	4.9	3544	4.1	3764
50	22.0	10,872	4.3	3860	3.4	3102	3.4	3420	2.0	2027
60	20.0	9947	4.3	3856	3.4	3386	3.4	3277	2.1	2062

macroporosity values in 0- to 10-cm and 20- to 30-cm layers were 2.2% and 2.5% respectively in P1, and that values in 0- to 10-cm and 20- to 30-cm layers were 0.3% and 0.9% respectively in highly compacted P4 (Fig. 4), which suggested that compaction in mine dump caused more severe damage not only to the soils but also to the vegetation growth and effect of reclamation. Therefore, care need to be taken to minimize the significant detrimental impacts of soil compaction in coal mine dumps.

Soil compaction affects not only soil properties but also local environment, resulting in the degradation of soil functions such as water heat exchange, carbon and nitrogen cycling capacity, and the deterioration of local environment such as emissions of greenhouse gases (N_2O , CH_4 , and CO_2) and vegetation cover reduction (Nawaz et al. 2013). Soil pore condition can be a related factor to activities of plant roots (Emerson and McGarry 2003). Proper quantification of soil compaction effects is essential to develop management strategies that minimize the harmful compactive effects. In the compacted sites of this study, soil porosities are less than 10%, which is expected to significantly alter the ability of plants to grow in waste dumps.

4.4 Implications for soil compaction impacts and recovery on opencast mine soils

In order to achieve the natural conditions of soil profile like P0, land reclamation is encouraged in the mining area. Natural recovery of compacted soils is a very complex and slow process (Froehlich et al. 1985), and the level of compaction or bulk density is the most important factor to monitor during the soil recovery period (Heinonen 1977). Over a 20-year period of reclamation time, with the application of soil amendments, soil pore structure can be improved and vegetation cover can be increased (Wang et al. 2016), but full recovery time for a heavy compacted soil can range from 100 to 190 years (Webb 2002). Therefore, two measures, in mining area, can be used to prevent soil compaction: (1) minimizing soil compaction during the operation of large machinery and (2) improving soil recovery effects by deep tillage, fertilizer application, etc. Natural phenomena involved are precipitation, wetting and drying cycles, subsequent soil cracking, and bioturbation in the recovery of compacted soils (Webb 2002; Drewry 2006). Compaction can be reduced by the artificial and natural methods through the increase of vegetation and addition of organic matter by the aforementioned solutions; therefore, both of these recovery methods are encouraged and employed in opencast coal mine dump sites.

Although the results of this study reveal the effects of large machinery compaction on dump soils, further studies on the mine soil hydraulic properties and the soil water migration pattern are still needed.

5 Conclusions

This study described the results from four sampling sites at dumping area in opencast coal mine, with different compaction level caused by large machinery, based on non-destructive computed tomography (CT), three-dimensional reconstruction software VGStudio, and Minkowski theory. The soil compaction significantly changed the soil properties and pore structure. Soil pore morphological indices, VD, SD, and MCD decreased with increasing soil compaction level, and they decreased from 0.10–0.20, 2.23–2.81 $mm^2 mm^{-3}$, and 10.75–15.64 $mm mm^{-3}$ respectively in P0 to 0.02–0.07, 0.13–0.60 $mm^2 mm^{-3}$, and 1.61–4.27 $mm mm^{-3}$ respectively in P4. In addition, EN increased with increasing compaction level, and it increased from 28,878–129,861 in P0 to 1,169,967–2,281,998 in P4. The results also demonstrated that CT-based method was a valuable tool for the quantification of compacted soil pores in mining area. Analysis based on Minkowski functionals indicated that the microstructure of compacted soil had been severely destroyed, thus the reconstruction of soil should be given more consideration. Due to the great contributions of soil pores in determining soil transport, aeration, and fertility, it is predicted that the undisturbed soils would respond more favorably to land reclamation than the compacted soils.

Funding This research was supported by the National Natural Science Foundation of China (41271528), Beijing Higher Education Young Elite Teacher Project (YETP0638), and the Fundamental Research Funds for the Central Universities of China (2652017002).

References

- Amer AMM, Logsdon SD, Davis D (2009) Prediction of hydraulic conductivity as related to pore size distribution in unsaturated soils. *Soil Sci* 174:508–515
- Anderson SH, Peyton RL, Gantzer CJ (1990) Evaluation of constructed and natural soil macropores using X-ray computed tomography. *Geoderma* 46:13–29
- Arns CH, Knackstedt MA, Mecke KR (2002) Characterising the morphology of disordered materials. *Lect Notes Phys* 600:37–74
- Bai ZK, Wang WY, Li JC, Lu CE (1998) Ecological rehabilitation of drastically disturbed land at large opencut coal mine in loess area. *Chin J Appl Ecol* 9:621–626
- Barik K, Canbolat MY, Yanik R, Islam KR (2011) Compressive behavior of soil as affected by aggregate size with different textures in Turkey. *J Anim Plant Sci* 21:186–192
- Beven K (1981) Micro, meso, macroporosity and channeling flow phenomena in soils. *Soil Sci Soc Am J* 45:97–106
- Beylich A, Oberholzer HR, Schrader S, Hoper H, Wilke BM (2010) Evaluation of soil compaction effects on soil biota and soil biological processes in soils. *Soil Tillage Res* 109:133–143
- Bi RT, Bai ZK, Li H, Shao HB, Li WX, Ye BY (2010) Establishing a clean-quality Indicator system for evaluating reclaimed land in the Antaibao opencast mine area, China. *Clean Soil Air Water* 38:719–725

- Blake G, Hartge K (1986) Particle density. *Methods of soil analysis: part 1—physical and mineralogical methods*, pp 377–382
- Bouma J, Jongerius A, Boersma O, Jager A, Schoonderbeek D (1977) The function of different types of macropores during saturated flow through four swelling soil horizons. *Soil Sci Soc Am J* 41:945–950
- Cnudde V, Boone MN (2013) High-resolution X-ray computed tomography in geosciences: a review of the current technology and applications. *Earth-Sci Rev* 123:1–17
- Cortina-Januchs MG, Quintanilla-Dominguez J, Vega-Corona A, Tarquis AM, Andina D (2011) Detection of pore space in CT soil images using artificial neural networks. *Biogeosciences* 8:279–288
- Silva AP, Imhoff S, Corsi M (2003) Evaluation of soil compaction in an irrigated short-duration grazing system. *Soil Tillage Res* 70:83–90
- Dauda A, Samari A (2002) Cowpea yield response to soil compaction under tractor traffic on a sandy loam soil in the semi-arid region of northern Nigeria. *Soil Tillage Res* 68:17–22
- Drewry JJ (2006) Natural recovery of soil physical properties from treading damage of pastoral soils in New Zealand and Australia: a review. *Agric Ecosyst Environ* 114:159–169
- Drewry JJ, Cameron KC, Buchan GD (2008) Pasture yield and soil physical property responses to soil compaction from treading and grazing - a review. *Aust J Soil Res* 46:237–256
- Emerson WW, McGarry D (2003) Organic carbon and soil porosity. *Aust J Soil Res* 41:107–118
- Frick J, Degenhardt B, Buchecker M, Hunziker M, Clivaz C, Siegrist D (2007) Predicting local residents' use of nearby outdoor recreation areas through quality perceptions and recreational expectations. *For Snow Landsc Res* 81:31–41
- Froehlich HA, Miles DWR, Robbins RW (1985) Soil bulk-density recovery on compacted skid trails in Central Idaho. *Soil Sci Soc Am J* 49:1015–1017
- Goodwin AK, O'Neill MA, Anderson WF (2003) The use of X-ray computer tomography to investigate particulate interactions within open-cast coal mine backfills. *Eng Geol* 70:331–341
- Greacen EL, Sands R (1980) Compaction of forest soils. A review. *Aust J Soil Res* 18:163–189
- Hamza MA, Anderson WK (2003) Responses of soil properties and grain yields to deep ripping and gypsum application in a compacted loamy sand soil contrasted with a sandy clay loam soil in Western Australia. *Aust J Agric Res* 54:273–282
- Haralick RM, Shapiro LG (1985) Image segmentation techniques. *Comput Vision Graph* 29:100–132
- Heinonen R (1977) Towards “normal” soil bulk density. *Soil Sci Soc Am J* 41:1214–1215
- Horn R, Domzal H, Slowinskajurkiewicz A, Vanouwerkerk C (1995) Soil compaction processes and their effects on the structure of arable soils and the environment. *Soil Tillage Res* 35:23–36
- Iassonov P, Gebrenegus T, Tuller M (2009) Segmentation of X-ray computed tomography images of porous materials: a crucial step for characterization and quantitative analysis of pore structures. *Water Resour Res* 45(9). <https://doi.org/10.1029/2009WR008087>
- Katuwal S, Norgaard T, Moldrup P, Lamande M, Wildenschild D, de Jonge LW (2015) Linking air and water transport in intact soils to macropore characteristics inferred from X-ray computed tomography. *Geoderma* 237:9–20
- Kim H, Anderson SH, Motavalli PP, Gantzer CJ (2010) Compaction effects on soil macropore geometry and related parameters for an arable field. *Geoderma* 160:244–251
- Krummelbein J, Horn R, Raab T, Bens O, Huttel RF (2010) Soil physical parameters of a recently established agricultural recultivation site after brown coal mining in eastern Germany. *Soil Tillage Res* 111:19–25
- Kumar S, Anderson SH, Udawatta RP, Gantzer CJ (2010) CT-measured macropores as affected by agroforestry and grass buffers for grazed pasture systems. *Agrofor Syst* 79:59–65
- Lehmann P, Wyss P, Flisch A, Lehmann E, Vontobel P, Krafczyk M, Kaestner A, Beckmann F, Gygi A, Fluhler H (2006) Tomographical imaging and mathematical description of porous media used for the prediction of fluid distribution. *Vadose Zone J* 5:80–97
- Li H, Shao HB, Li WX, Bi RT, Bai ZK (2012) Improving soil enzyme activities and related quality properties of reclaimed soil by applying weathered coal in open-cast-mining areas of the Chinese Loess Plateau. *Clean Soil Air Water* 40:233–238
- Lipiec J, Hatano R (2003) Quantification of compaction effects on soil physical properties and crop growth. *Geoderma* 116:107–136
- Luxmoore R (1981) Micro-, meso-, and macroporosity of soil. *Soil Sci Soc Am J* 45:671–672
- McGarry D, Sharp G (2003) A rapid, immediate, farmer-usable method of assessing soil structure condition to support conservation agriculture. *Conservation agriculture*. Springer, Netherland, pp 375–380
- Mecke KR (2000) Additivity, convexity, and beyond: applications of Minkowski functionals in statistical physics. Springer, Berlin, Heidelberg, pp 111–184
- Meng C, Niu JZ, Li X, Luo ZT, Du XQ, Du J, Lin XN, Yu XX (2017) Quantifying soil macropore networks in different forest communities using industrial computed tomography in a mountainous area of North China. *J Soils Sediments* 17:2357–2370
- Mueller L, Schindler U, Mirschel W, GrahamShepherd T, Ball BC, Helming K, Rogasik J, Eulenstein F, Wiggering H (2010) Assessing the productivity function of soils. A review. *Agron Sustain Dev* 30:601–614
- Naveed M, Moldrup P, Schaap MG, Tuller M, Kulkarni R, Vogel HJ, de Jonge LW (2016) Prediction of biopore- and matrix-dominated flow from X-ray CT-derived macropore network characteristics. *Hydrol Earth Syst Sci* 20:4017–4030
- Nawaz MF, Bourrie G, Trolard F (2013) Soil compaction impact and modelling. A review. *Agron Sustain Dev* 33:291–309
- Oni KC, Adeoti JS (1986) Tillage effects on differently compacted soil and on cotton yield in Nigeria. *Soil Tillage Res* 8:89–100
- Osullivan MF, Simota C (1995) Modeling the environmental impacts of soil compaction - a review. *Soil Tillage Res* 35:69–84
- Pal NR, Pal SK (1993) A review on image segmentation techniques. *Pattern Recogn* 26:1277–1294
- Panayiotopoulos KP, Papadopoulou CP, Hatjioannidou A (1994) Compaction and penetration persistence of an alfisol and entisol and their influence on root-growth of maize seedlings. *Soil Tillage Res* 31:323–337
- Rab MA, Haling RE, Aarons SR, Hannah M, Young IM, Gibson D (2014) Evaluation of X-ray computed tomography for quantifying macroporosity of loamy pasture soils. *Geoderma* 213:460–470
- Rachman A, Anderson SH, Gantzer CJ (2005) Computed-tomographic measurement of soil macroporosity parameters as affected by stiff-stemmed grass hedges. *Soil Sci Soc Am J* 69:1609–1616
- Rasiah V, Aylmore LAG (1998) Characterizing the changes in soil porosity by computed tomography and fractal dimension. *Soil Sci* 163:203–211
- San José Martínez F, Martín MA, Caniego FJ, Tuller M, Guber A, Pachepsky Y, García-Gutiérrez C (2010) Multifractal analysis of discretized X-ray CT images for the characterization of soil macropore structures. *Geoderma* 156:32–42
- San José Martínez F, Muñoz Ortega FJ, Caniego Moreal FJ, Peregrina F (2016) Morphological functions with parallel sets for the pore space of X-ray CT images of soil columns. *Pure Appl Geophys* 173:995–1009
- Schluter S, Leuther F, Vogler S, Vogel HJ (2016) X-ray microtomography analysis of soil structure deformation caused by centrifugation. *Solid Earth* 7:129–140
- Schneider CA, Rasband WS, Eliceiri KW (2012) NIH image to ImageJ: 25 years of image analysis. *Nat Methods* 9:671–675

- Sezgin M, Sankur B (2004) Survey over image thresholding techniques and quantitative performance evaluation. *J Electron Imaging* 13: 146–168
- Shukla MK, Lal R, Underwood J, Ebinger M (2004) Physical and hydrological characteristics of reclaimed minesoils in southeastern Ohio. *Soil Sci Soc Am J* 68:1352–1359
- Soane BD (1990) The role of organic-matter in soil compactibility - a review of some practical aspects. *Soil Tillage Res* 16:179–201
- Soracco CG, Lozano LA, Villarreal R, Palancar TC, Collazo DJ, Sarli GO, Filgueira RR (2015) Effects of compaction due to machinery traffic on soil pore configuration. *Rev Bras Cienc Solo* 39:408–415
- Taina IA, Heck RJ, Elliot TR (2008) Application of X-ray computed tomography to soil science: a literature review. *Can J Soil Sci* 88: 1–20
- Taylor JH (1992) Reduction of traffic-induced soil compaction - special issue. *Soil Tillage Res* 24:301–302
- Udawatta RP, Gantzer CJ, Anderson SH, Garrett HE (2008) Agroforestry and grass buffer effects on pore characteristics measured by high-resolution X-ray computed tomography. *Soil Sci Soc Am J* 72:295–304
- Vogel HJ (2000) A numerical experiment on pore size, pore connectivity, water retention, permeability, and solute transport using network models. *Eur J Soil Sci* 51:99–105
- Vogel HJ, Weller U, Schluter S (2010) Quantification of soil structure based on Minkowski functions. *Comput Geosci* 36:1236–1245
- Wang JM, Guo LL, Bai ZK, Yang LL (2016) Using computed tomography (CT) images and multi-fractal theory to quantify the pore distribution of reconstructed soils during ecological restoration in opencast coal-mine. *Ecol Eng* 92:148–157
- Wang JM, Guo LL, Bai ZK (2017a) Variations in pore distribution of reconstructed soils induced by opencast mining and land rehabilitation based on computed tomography images. *Arch Agron Soil Sci* 63:1685–1696
- Wang JM, Yang RX, Feng Y (2017b) Spatial variability of reconstructed soil properties and the optimization of sampling number for reclaimed land monitoring in an opencast coal mine. *Arab J Geosci* 10:46
- Warner GS, Nieber JL, Moore ID, Geise RA (1989) Characterizing macropores in soil by computed-tomography. *Soil Sci Soc Am J* 53:653–660
- Webb RH (2002) Recovery of severely compacted soils in the Mojave Desert, California, USA. *Arid Land Res Manag* 16:291–305
- Williamson JR, Neilsen WA (2000) The influence of forest site on rate and extent of soil compaction and profile disturbance of skid trails during ground-based harvesting. *Can J For Res* 30:1196–1205
- Worrell R, Hampson A (1997) The influence of some forest operations on the sustainable management of forest soils - a review. *Forestry* 70: 61–85
- Xu YJ, Burger JA, Aust WM, Patterson SC, Miwa M, Preston DP (2002) Changes in surface water table depth and soil physical properties after harvest and establishment of loblolly pine (*Pinus taeda* L.) in Atlantic coastal plain wetlands of South Carolina. *Soil Tillage Res* 63:109–121